

# INSTRUMENTAL QUANTIFICATION OF SUBJECTIVE FORMATION

**R. J. HALL, Wiggins Teape Research & Development Ltd.,  
Beaconsfield, Bucks.**

---

**Synopsis** The means of defining formation in terms of its subjective appearance was explored by processing the transmitted light signal from various paper samples on an analogue computer using equations related to physiological attributes. Some psychological aspects of the interpretation of images are discussed and the relevant aspects of both of these is described. It is demonstrated how this approach was implemented in an instrumental technique to quantify hitherto subjective assessments of quality.

The statistical significance of the aspects of microformation and macroformation is explained and practical analysis is achieved by dissecting an area into strips. The value of each strip is derived from the content of the microformation, these values are then analysed for mean and standard deviation to assign numbers for both the microformation and macroformation. The instrument outputs a weighted value of the sum of the two figures on a continuous sampling basis.

The instrument has been used in the laboratory for sample testing, in particular cigarette tissue, also on a papermachine making tracing paper, where a continuous record is produced.

## **Definition of formation**

THE formation of paper is a visual attribute that is important in various specific paper types. Examples of these are usually found in lightweight and consequently semi-transparent papers, for which cloudy or blotchy appearance will detract from the product, be it the paper itself or the legibility of characters or designs printed upon it.

This paper is intended to present a new approach to the definition of formation in terms of its subjective appearance and to show how this approach can be implemented in an instrumental technique to quantify hitherto subjective (consequently, inaccurate and inconsistent) assessments of quality.

*Inaccurate and inconsistent*, because we are using our eyes! The term 'seeing is believing' has long been disproved in two very common present-day

*Under the chairmanship of Dr J. D. Peel*

situations—the cinema, where a rapid presentation of series of still pictures presents the illusion of a continuity of movement; the even more surprising situation of seeing a moving picture where, in fact, no picture exists—television! We all see it and take it for granted.

Both of these examples rely for their deception of the eye upon one of its attributes—the persistence of vision. Experiments have shown that the presentation of pictures in this intermittent form is, in all possibility, an extension of one of the eye's natural operations. Gregory<sup>(1)</sup> describes an experiment in which it is proved that 'seeing' is achieved by a continuous comparison of each small part of the image formed on the retina by its adjacent part. If an image is fixed on the retina so that, whenever the eye moves the image moves with it, it is found that after a few seconds the object could no longer be seen. It simply fades away!

There is also a psychological aspect that plays an important and sometimes misleading part in the process of observing objects around us. Our observations and their interpretation are based upon a continuous process of learning that starts in infancy and becomes a source of reference for interpretation and motive functions. The presentation of a picture of a person's face upsidedown is so unfamiliar that recognition is difficult and it is certainly impossible to judge facial expression. An automatic motivation is to rotate the picture or turn the head so that the brain may make an identification based upon historic reference.

This is not an irreversible process. The wearing of special glasses that cause the image on the retina to be erect instead of inverted, as is normal, initially create an upsidedown world. With continual wearing, the subject will eventually see right way up so that, when the glasses are removed, the upsidedown situation is again experienced.

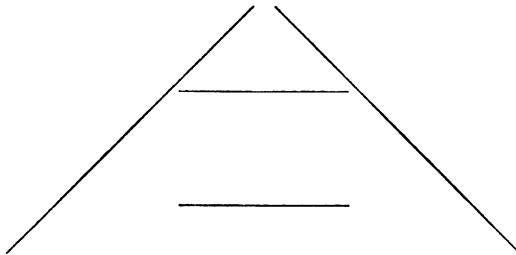


**Fig. 1**—Tramlines illusion

The brain also makes corrections for perspective so that the distorted picture received on the retina is interpreted as being three dimensional. Thus, the effect of depth is created in art and photography on a flat plane, because the brain associates these visual impressions in the same manner as real life

situations. The brain is thus open to deception by using these guidelines in circumstances to which the rules do not apply. Optical illusions arise from this cause as illustrated in Fig. 1: two horizontal lines of equal length are interpreted as being at different distances from the observer, consequently the line apparently furthest away is registered as longer.

### ***Quantifying formation***

IN THE attempt to quantify the appearance of paper formation, it is of importance to include the factors of perception that come into play and the weightings associated with these factors.

In the process of assessing paper formation, a judgment is made whether the paper is better or worse from a psychological impression. What is good and bad formation? A contradiction arises when a bond paper is judged bad if the appearance is mottled instead of smooth, whereas a ceiling paper with a mottled random pattern finish may be more acceptable than plain paper. So there is a concept of ugliness and beauty. The task of quantifying this aspect must thus take into account the popular concepts of formation quality.

Usually, the optical formation of paper is judged by observing the local variations in the intensity of light that has been transmitted through the sheet. The passage of a beam of light through the fibrous web is influenced by the changes of refractive index it encounters in the layers because of air, fibre and fillers causing absorption, scattering and refraction in a complex manner. This complex transmission pattern forms the light and dark areas seen by an observer.

In broad terms, a poor formation is when the sheet looks very blotchy on being held to the light; good formation is when there is little or no noticeable transmission variation.

The scale of these variations is important and has been measured on some instruments as a quasi-spatial frequency spectrum ranging  $\frac{1}{84}$ –2 in. This form of analysis is inconvenient as a continuous quality monitor and can be interpreted only by detailed examination of the results after the test. A further step would then be required to relate the results to the factors affecting human judgment and yet a further step to obtain a ranking. Considerable expertise is involved and the results do not produce a definitive number.

The first step in approaching this problem is to fix the zero of the formation scale. If zero is defined as perfect formation, we have the concept of a numeric scale that must relate to formation in the accepted psychological sense, the scale arranged so that a worsening formation is indicated by an increase in magnitude. Based upon this premise, the definition of zero optical formation may thus be stated as a 'sheet of translucent material that has zero perceptible variations in light transmission over its entire area has zero formation.'

This definition takes into account the spatial bandwidth of vision. The short wavelength restriction is given by Helmholtz as a maximum eye resolution of 50 s of arc for the half angle, which at the least distance of distinct vision subtends a half wavelength of  $61.6 \mu\text{m}$ . The long wavelength cannot be defined in this way, as there is no optimum object to eye distance. Thus, objects the size of the earth can be resolved with the eye focused at infinity and when the object distance is very great.

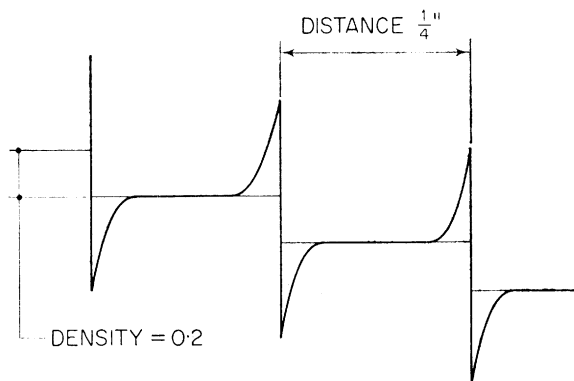


**Fig. 2**—Step wedge illusion

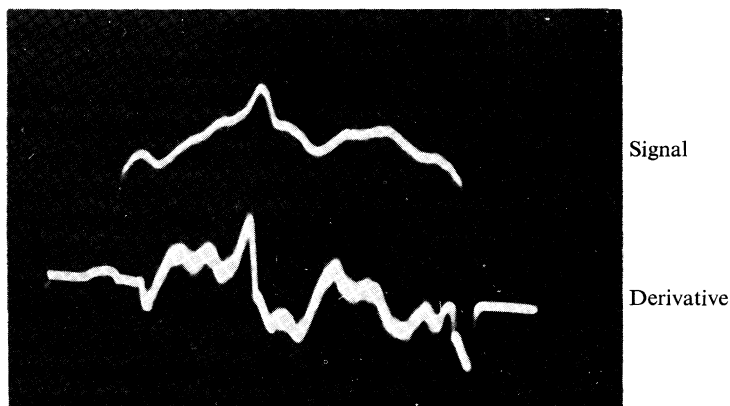


**Fig. 3**—(Upper) Oscillograph of formation scan  
(Lower) Processed derivative

Andersson & Sundwall<sup>(2)</sup> performed an experiment with photographic plates that had been exposed so that, in the first case, smooth variation of photographic density from one edge of the plate to the other was obtained:



in the second case, two halves of the plate were exposed for different times to give a density difference equal to the total variation in the first plate. Several observers when asked their opinion could detect with ease the step variation of the second plate, but could not recognise any variation in light intensity across the first plate.

The observations of E. Mach published in 1844 illustrate that a mental sharpening of an image takes place when the density gradient is high. This effect is quite noticeable when looking at a transparent step wedge in which the steps have been measured by a microdensitometer as being uniform. It is observed that, in the direction of increasing step density, each density plateau appears to start at high density, diminish at first fairly rapidly, then less rapidly and ending at the step junction as a sudden decrease in density. This is a precisely similar phenomenon to Mach's rings without the possibility of a flicker effect. By comparing the apparent density with known densities of a larger area, the curve (Fig. 2) of real density and apparent density is shown. This graph shows that the enhancement extends on either side of the point of inflexion and continues over regions of zero slope. The complexity of the image dissection is shown by Mach's ring, where the effect is circular, thus precluding lineal retinal movement and suggesting a process of adjacent cell differentiation and enhancement.

The eye is thus conditioned by rates of change of image brightness. It is suggested therefore that the condition of a density gradient being only just discernible could form the basis of a definition for the long wavelength spatial bandwidth limitation of vision.

Another effect, the Weber-Fechner law, which states that the eye stimulus  $E_s$  is equal to the logarithm of  $S$ , the light flux, is also present in the observation of the regions of light and dark. For a homogeneous light absorber, the light flux is proportional to the mean transmission  $T$  and as  $\log_{10} T = -D$ , where  $D$  is the optical density due to a linear increase of material thickness—

$$S \propto T = 10^{-D}$$

The eye stimulus  $E_s = \log S$ .

Thus,  $E_s = \log S \propto \log T = -D$  so  $E_s \propto -D$ .

### **Instrumental quantification**

INSTRUMENTALLY, it is usual to maintain the mean value of  $S$  constant, usually by controlling the strength of the illuminator. This has the effect of centralising one point of the logarithmic curve to give a semi-constant slope for all the variations due to formation. It is quite usual for this variation to be a small fraction of the mean transmitted light. Consequently, it is usual to process the signal in a linear manner.

Having established a definition for zero formation, this can be standardised in terms of a diffusing screen with no perceptible variation of intensity within its boundaries. The next step is to introduce an instrumental technique that will incorporate various aspects of visual perception, thereby to obtain a final result that will agree with a statistically determined visual impression.

Firstly, the eye dissects the image into a cellular form. This method is complex with the problem of handling a multiplicity of parallel analogue information. Simplification is essential and may be reduced to a single dimension by using one cell that is moved rapidly so that an area of paper equivalent to twenty stationary cells is scanned serially. This is achieved in practice by the use of a small aperture through which the transmitted light is gathered, then measured with a linear light-sensitive receiver, typically a photomultiplier.

This small aperture is made to move across the paper surface in order to obtain the spatial variation of the transmitted light and results in a varying electric current, which represents a microprofile of the formation. A human eye sees a small difference between adjacent elements and the difference is emphasised. The corresponding change in current between the adjacent elements detected by the instrument must be emphasised in a similar way. The process of dynamically scanning the paper with a flying image of this type causes a conversion from the spatial frequency of the paper to a temporal frequency of the electronic signal and this is convenient as analogue operational functions must be performed in the time domain.

The emphasis is carried out by extracting the derivative of the electronic signal (Fig. 3). The speed of scan is important.

As  $L = f(S, T)$  where  $L$  = light flux,

$S$  = linear distance,

$T$  = paper transmission.

$$\frac{\partial L}{\partial S} \cdot \frac{\partial S}{\partial t} = \frac{\partial f(T)}{\partial S} \cdot \frac{\partial S}{\partial t}$$

$$\frac{\partial L}{\partial t} = \frac{\partial f(T)}{\partial t} \quad \text{only when} \quad \frac{\partial S}{\partial t} = \text{constant.}$$

Thus, the scan speed  $\partial S/\partial t$  must be made substantially constant for all web speeds. This is achieved by using a high constant speed scan in the web cross-direction. The velocity vector that arises when the paper is moved is shown in Fig. 4. The increase in the resultant velocity  $R$  above the scan velocity  $S$  is simply—

$$\frac{\dot{R}}{\dot{S}} = \left( \text{Sectan}^{-1} \frac{\dot{P}}{\dot{S}} \right)^{-1}$$

The scan rate  $S$  is fixed in the instrument at 2 000 m/min, which results in an

increase of only 1.12 per cent when the paper velocity is increased from zero up to 300 m/min.

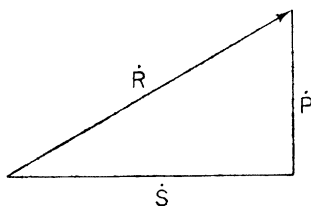


Fig. 4—Velocity triangle

Microformation begins to become objectionable at clump spacings of about 1 mm apart, which in terms of wavelength is 2 mm. The size of the interrogating aperture will determine the shortest wavelengths of interest, provided there are no other bandwidth constraints within the electronic processor. The short wave cut-off characteristics of an aperture were discussed by Moen<sup>(3)</sup> and are shown in Fig. 5. Here, the parameter  $A$  is some suitable measure of probe size such as diameter or slit width. A 1 mm square aperture was chosen to give a short wave attenuation above 2 mm wavelengths.

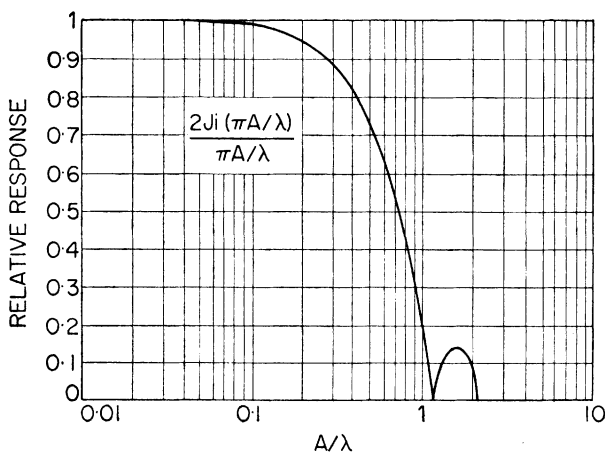


Fig. 5—Aperture cut-off characteristics (after Moen)

The long wave cut-off is determined by the combination of the aperture and the electronic derivative extraction of the signal. A characteristic rise of 6 dB per octave is obtained by differentiation and this must be combined with the curve for the aperture restriction to obtain the spatial bandwidth. When this is done, the theoretical curve (Fig. 6) shows that considerable filtering of the

signal wavelengths occurs, producing a peak response at  $A/\lambda = 0.6$ , which in our case, with a 1 mm aperture, occurs at a wavelength of 1.66 mm. In addition, harmonic lobes present in the aperture filter are emphasised to an undesirable extent. They are removed in the design by converting the analogue differentiator into a single stop differentiator by adding an asymptote of the form  $(1 + \omega^2 T^2)^{-\frac{1}{2}}$  to the Bode diagram. The Bode function  $\omega$  now becomes—

$$G(\omega) = \omega T(1 + \omega^2 T^2)^{-\frac{1}{2}}$$

and the break point  $\omega = 1/T$  is selected near the main peak of Fig. 6 at  $A/\lambda = 0.5$ .

The combined wavelength response thus becomes—

$$f(\lambda) = 20 \log_{10} \omega T - 10 \log_{10} (1 + \omega^2 T^2) + 20 \log 2J_1 \left( \frac{\pi A}{\lambda} \right) / (\pi A/\lambda)$$

where  $\omega = 2\pi(\dot{R})/\lambda$  and is shown normalised in Fig. 7.

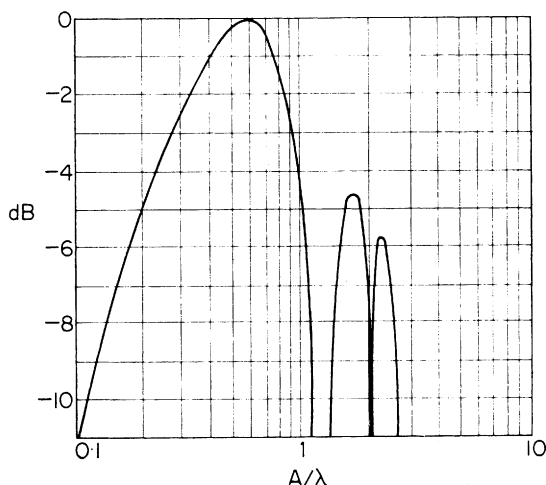


**Fig. 6**—Combined signal filtering due to aperture and differentiation

The 3 dB bandwidth of the system is thus confined to wavelengths between 1.31 mm and 5 mm.

The combined curve of spatial bandwidth of the instrument now relates to the spatial bandwidth of vision for small changes in intensity.

The next problem is how to process the eye-filtered electronic signal, which is occurring as a time varying analogue voltage during each scan of the flying image. Various processing equations (Fig. 8) were tried upon graded samples

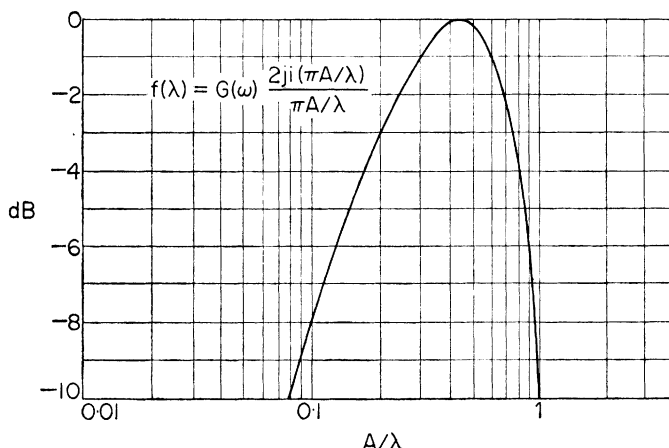


Fig. 7—Signal filtering with correction applied

using an analogue computer. The most promising was equation (6) and, to simplify the electronics, a modified form of this was adopted that measures the area under the derivative curve relative to the most negative going peak (Fig. 9).<sup>\*</sup> Of necessity, a time constant is introduced into this measurement and this is adjusted to account for yet a further subjective factor. In judging formation, the observer will not relate the imperfections to the quality in a linear manner. This is exemplified by a particular weighting that the observer places upon the ratio between unblemished to blemished areas. When scanning paper, the observer is attracted to the blemished areas and they are then sub-consciously weighted against the area under consideration.

Consider two papers of uniform formation, for example, to the first (Fig. 10) type, we will assign the number 1 and to the second type, which has a more intense mottle, but of the same wavelength, the arbitrary number 10. Now, if we introduce a third paper that has an area of 50 per cent of each type, the observer will not usually assign a number 5.5, corresponding to 50 per cent of 1 + 50 per cent of 10. In most probability, the combination will be judged as equally bad or worse than the second type. Thus, isolated spatial disturbances will produce disproportionately larger subjective disturbances.

<sup>\*</sup> A dc restoration circuit is used that senses negative excursions of the signal and subtracts this negative value from succeeding signals. This is followed by an integrator operating within the time limits  $t_1 t_2$ .

The processing equation for  $f$  is thus—

$$f = \int_{t_1}^{t_2} \left[ \frac{dx}{dt} - \left( \frac{dx}{dt} \min \epsilon^{-t/CR} \right) \right] dt \quad \text{where } 0 > \frac{dx}{dt} \min > -\infty$$

## OPERATION

$$\left[ \frac{1}{T_0} \int_0^{T_0} x^2 dt \right]^{\frac{1}{2}} \quad \text{(RMS of)} \quad . \quad . \quad . \quad . \quad . \quad . \quad . \quad . \quad . \quad (1)$$

$$\left( \frac{1}{T_0} \int_0^{T_0} \frac{d}{dt} \log x^2 dt \right)^{\frac{1}{2}} \quad \text{RMS of } \frac{d}{dt} \log x \quad . \quad . \quad . \quad . \quad . \quad . \quad . \quad . \quad . \quad (2)$$

$$\left( \frac{1}{T_0} \int_0^{T_0} \frac{d}{dt} x^2 dt \right)^{\frac{1}{2}} \quad \text{RMS of } \frac{dx}{dt} \quad . \quad . \quad . \quad . \quad . \quad . \quad . \quad . \quad . \quad (3)$$

$$\left( \frac{1}{T_0} \int_0^{T_0} \frac{d}{dt} \log (K-x)^2 dt \right)^{\frac{1}{2}} \quad \text{RMS of } \frac{d}{dt} \log (K-x) \text{ to simulate reflectance} \quad . \quad . \quad . \quad (4)$$

$$\left( \frac{1}{T_0} \int_0^{T_0} \left| \frac{dx}{dt} \right| dt \right)^{\frac{1}{2}} \quad \text{Root of average modulus value of } \frac{dx}{dt} \quad . \quad . \quad . \quad . \quad (5)$$

$$\frac{1}{T_0} \int_0^{T_0} \left| \frac{dx}{dt} \right| dt \quad \text{Average modulus value of } \frac{dx}{dt} \quad . \quad . \quad . \quad . \quad . \quad . \quad (6)$$

$$\frac{1}{T_0} \int_0^{T_0} \left| \log \left( K - \frac{dx}{dt} \right) \right| dt \quad \text{Log derivative} \quad . \quad . \quad . \quad . \quad . \quad . \quad . \quad (7)$$

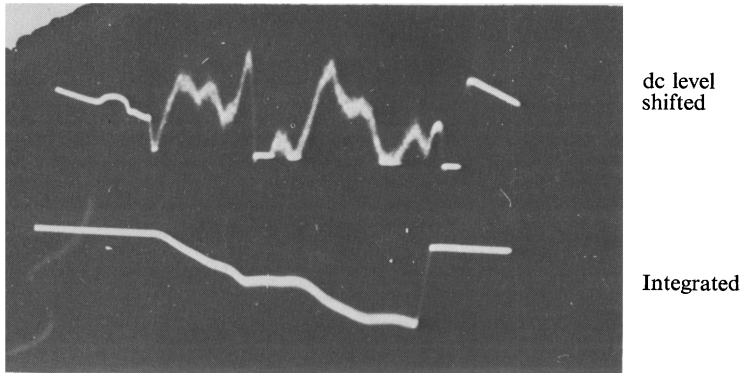
$$\frac{1}{T_0} \int_0^{T_0} \left| \frac{d}{dt} \log \left( K - \frac{dx}{dt} \right) \right| dt \quad \text{Derivative of (7)} \quad . \quad . \quad . \quad . \quad . \quad . \quad . \quad (8)$$

$$\frac{1}{T_0} \int_0^{T_0} |x| dt \quad \text{Average modulus} \quad . \quad . \quad . \quad . \quad . \quad . \quad . \quad (9)$$

**Fig. 8**—Permutations of eye processing equations

The time constant of the signal baseline will thus compensate to some degree for the larger peaks overshadowing smaller variations within a distance of 10 mm.

Finally, the areas above the peak negative values are integrated and the value at the end of the line scan is put into a store, where it remains for the



$$f = \bar{x} + 3\sigma$$

**Fig. 9—**(Upper) Derivatives with correction  
(Lower) Final integration

duration of a subsequent scan. The first compensation takes place within the line scan; further variations between lines must also be taken into account.

Two papers with dissimilar formation are shown in Fig. 11–13. The scanning technique described will divide the areas into strips, the variation along a strip is then summed to produce a number for the strip. By way of illustration, the contrast of each photograph has been increased and a grid superimposed to obtain discrete white spots so that the number of spots in each strip may be counted. This is not the process previously described, but is shown merely to illustrate how the data obtained relates to the appearance.

The counts for all of the columns are obtained for the two samples and the two histograms show the frequency distribution of these column counts. Distribution difference illustrates the important conclusion that the macroformation is produced by variations of the microformation.

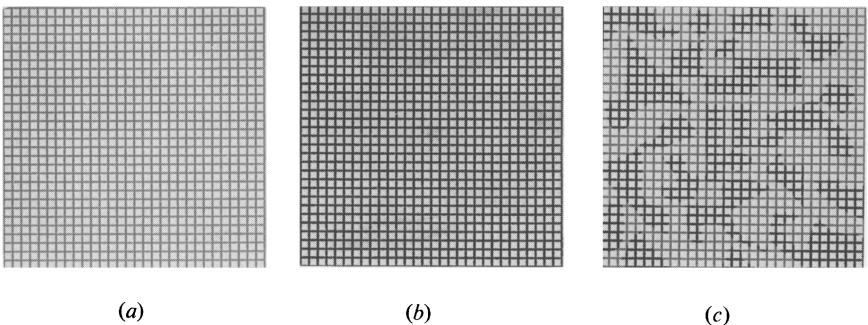
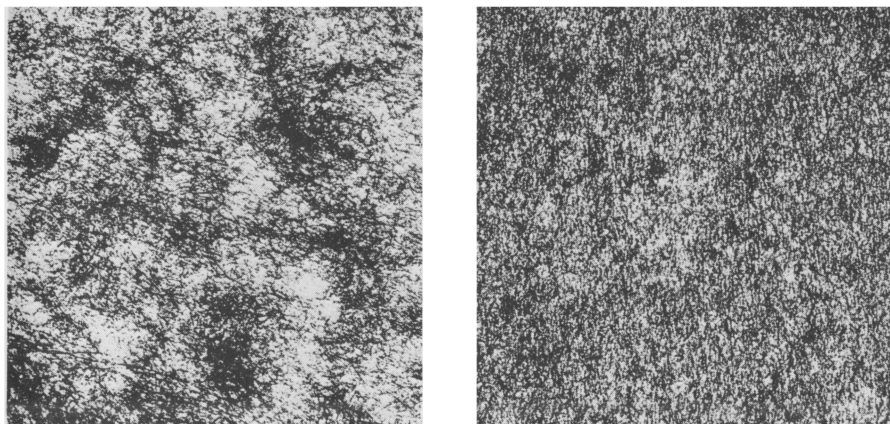


**Fig. 10—**Illustration of subjective weighting



(a)

(b)

**Fig. 11**—Formation in two dissimilar papers

A range of cigarette tissue formation samples of single type were submitted to experts for grading.

Submitting the samples to the instrument and plotting the values of single line scans produced histograms that showed the mean value of various grades to be altered very little, whereas the standard deviation increased with worsening grades (Fig. 14). Later tests with tracing paper produced a contrary result, greatest indication of worsening formation being indicated by the mean value, whereas the standard deviation remained static. The two papers serve to illustrate different formation property requirements, in which the tissue has a higher level of macroformation and the wet-beaten tracing paper has a very low level of macroformation and is judged mainly by its microformation intensity.

In order that the micro and macro data may be quantified, the statistic  $\bar{f} + 3\sigma$  was implemented in a hybrid calculator unit and incorporated into the instrument. Here,  $f$  is the value of each selected line scan. The mean value  $\bar{f}$  and standard deviation  $\sigma$  are computed from a sample of 64  $f$  readings.

Insertion of an  $f$  reading into the calculator is initiated by the passage of the paper over the scanning head through a distance of approximately 2 mm. This is independent of the scanning rate or paper speed, as an impulse generator is geared to the web movement and produces a command signal for the calculator to take one reading at each command pulse. Thus, 64 independent  $f$  readings are passed to the calculator, which computes  $\bar{f} + 3\sigma$ , then stores and displays this calculation on an analogue meter during the period of a subsequent calculation.



The  $f$  reading contains eye density response and some psychologic weightings. In order that standardisation on the numeric value of  $f$  can be realised, a test piece has been produced that can be measured by the instrument and to which all  $f$  readings can be related. This takes the form of a coarse grating whose spatial frequency is 1.3 mm, the line width is 0.15 mm and the line transmission density is 3.0. In use, the grating is placed with the lines at right-angles to the scan direction and backed with the zero formation diffusing screen. A calibration button is included on the instrument to reduce the sensitivity by half and, with this operated, the sensitivity is set so that a reading of  $f = 1.5$  corresponds to 15 calibrate lines per 2 cm window.

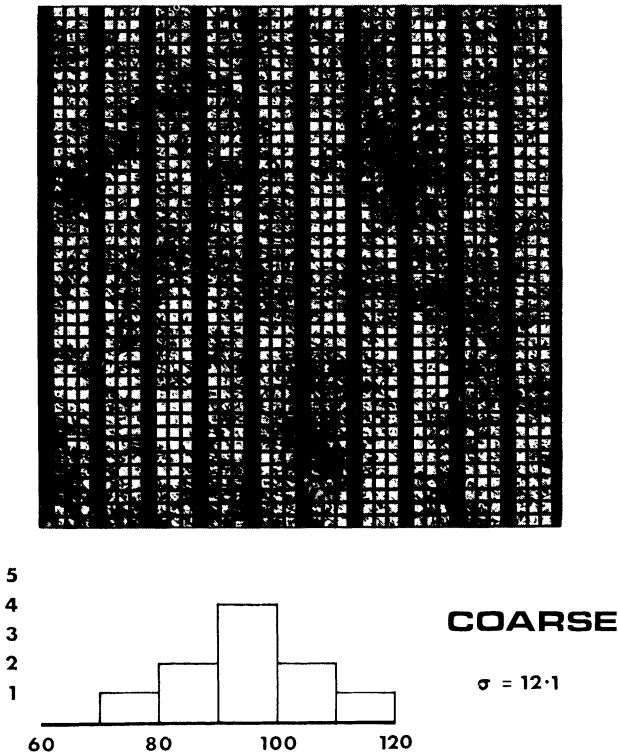
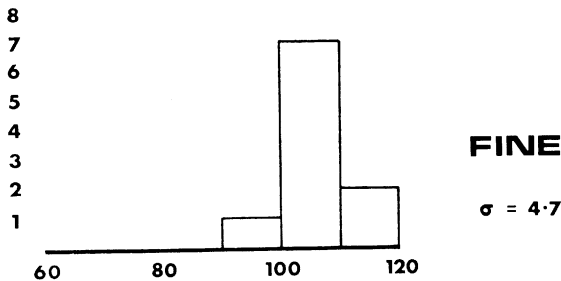


Fig. 12—Formation dissection for paper (a) Fig. 11 by scanning illustrating frequency distribution due to macroformation

### Applications

THE instrument was tested on 24 samples with differing formation and compared with the ranking of 40 observers. A Spearman rank correlation coefficient of 0.849 with 99.998 per cent confidence level was obtained.



**Fig. 13**—Formation dissection for paper (b) Fig. 11 by scanning illustrating frequency distribution due to macro-formation

In practice, the instrument has been used both in its laboratory form for testing cigarette tissue and on a papermachine making tracing paper.

Cigarette tissue is a difficult paper to measure, owing both to its varied forms of formation and to the laid lines and vergé markings usually present. The vergé lines are close spaced and run across the papermachine, whereas the laid lines are open spaced and run in the machine-direction. The vergé marking would produce a troublesome interference frequency if the scan is in the machine-direction, whereas the cross-direction scan of the instrument effectively eliminates this problem. Scanning across a laid line gives a greater reading and must be avoided whenever possible.

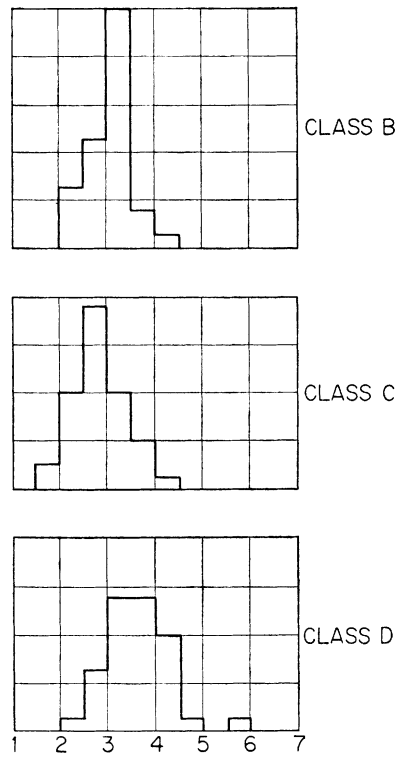


Fig. 14—Instrumental histogram of cigarette tissue

The results obtained on cigarette tissue are shown in Fig. 15 for 7 grades. Each point is an output reading from the calculator and represents a strip of paper 2 cm wide (the scan width) by 12.8 cm long (64 *f* readings, each at 2 mm spacing). The scatter of the readings indicates that there are considerable amounts of the same formation paper in various grades and that once again the high formation readings of a group are weighting the observer against the rest and moving the whole classification up. Discrimination against this

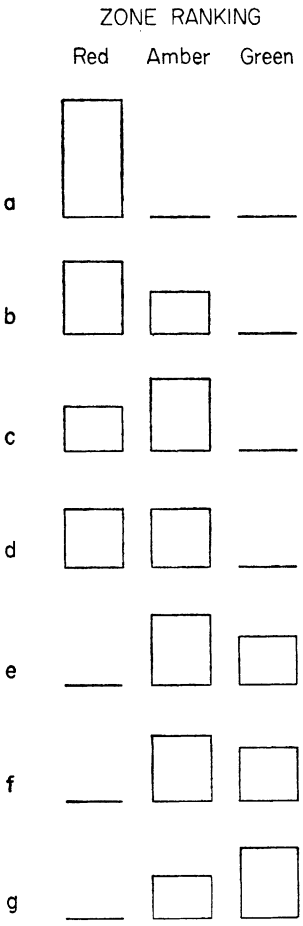
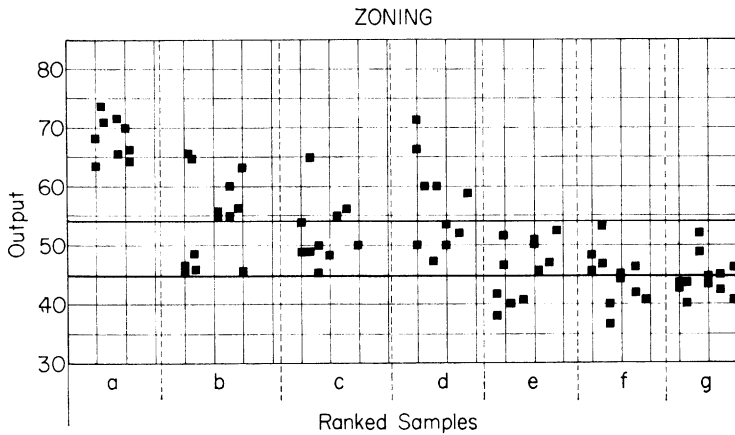


Fig. 16—Histogram of zone channel counts shows discrimination of ranks

may be made by introducing two zone limits and taking the ratio of the number of readings that fall in each zone. The instrument is fitted with two levels of selection into three zones and, by correct adjustment of these levels, it is possible to obtain the discrimination shown in Fig. 16. In this way, the zoning technique enables the formation capability to be extended to large lengths of paper to enable a general assessment of quality to be made by automatically counting the reading in each zone to permit the operator to take the ratio. Either the count could be reset at suitable distances or a continuous and equal subtraction from all three channels could be made.



**Fig. 15—** Calculator output values for different formation ranks  
Zoning limits selected as—  
Red—above 54    Amber—54 to 45    Green—below 45

Processing of this kind can be used to enable the instrument to measure complete cigarette tissue bobbins on a rewinding machine so that the classification of bobbin quality is not confined to end of bobbin samples.

Ultimately, the instrument would be best utilised direct on the paper-machine, where a suitable display could give the machine crew direct indication of the formation quality.

### References

1. Gregory, R. L., *Eye and Brain*
2. Andersson, O. and Sundewall, K., *Svensk Papperstidn.*, 1960, **63** (6), 167–173
3. Moen, C. J., *Tappi*, 1963, **46** (1), 34–37

## Transcription of Discussion

### *Discussion*

---

*The Chairman* From the lessons we have learned today and from the published work in the last few years, we may feel that we should restrict the use of the word *formation* to a visual subjective assessment, using *formation index* as a mathematical term. This may be one easy way of getting out of the confusion in which these terms have been used.

*Dr J. Grant* I notice Mr Hall that, in your Class D histogram (Fig. 12), the maximum frequency rectangle is derived from a single unit, whereas all your others are in half units. Is there any significance in this or does it just mean that there are two equal maxima?

*Mr R. J. Hall* That is precisely right. There are two maxima in histogram D.

*Mr C. M. W. Wilson* This is a comment (and only a rather minor comment) referring to the first paper this afternoon and to the paper earlier in the week by Scallan & Borch. Two people who have not come out of this week very well are Messrs. Kubelka and Munk—that's not personally, but in their application to the paper industry. I think it is well-established by what we have heard this week that the Kubelka-Munk scattering coefficient is purely a mathematical concept without very much physical meaning.

I would just like to redress the balance slightly by saying two things—first of all, the absorption coefficient in that theory *is* a physical value and, following on from that, many of us have for a long time found the Kubelka-Munk theory very useful in a number of respects, particularly in providing a theoretical parameter, for instance, for instrumental colour-matching systems. Although it may have certain theoretical and practical weaknesses, it has been and I am sure will continue to be of great practical use.

*Prof. D. Wahren* The very first restriction on the Kubelka-Munk equation mentioned by Dr Corte that it is valid only for a large surface, whose thickness is very small compared with its width, is not entirely correct. This assumption

*Under the chairmanship of Dr J. D. Peel*

## Discussion

was made by Kubelka and Munk, but it has been shown later that the same solution is in fact obtained with much less stringent requirements. The most stringent requirement on the area of the surface is that it should be much larger than the mean free path of photons between reflections. This is a very small distance.

The light diffusion as shown by Dr Corte is another kind of phenomenon.

I would like to make a remark to Mr Hall about the filtering theory by Moen shown in Fig. 5. The results there are in fact strictly valid only for parallel lines or for one-dimensional wave trains passing a circular aperture. I would refer to the paper 'Mass distribution and sheet properties of paper' (page 7), in which we demonstrate the influence of aperture when scanning two-dimensional structures.

*Prof. J. Silvy* I commented on the first day of this session about the use of Kubelka-Munk formulae, especially when the paper has a very high absorption for light. Theoretically, it is quite well established that the value of  $S$  is biased in this case compared with the true scattering coefficient such as can be computed using more accurate theories (and there are many of them, but much more sophisticated). The best way I think is to use a graph adapted to the specific problems.

The absorption coefficient  $K$  is more well defined than is the scattering coefficient and we have carried out many experiments giving proof that absorption can be estimated fairly well in diffusing media. The scattering coefficient, on the other hand, may be the result of some kind of artefact that depends on many parameters, especially the measuring device, the geometry of illumination, the calibration of the reflectometer, the making of the samples and so on. Fortunately, we have so many parameters that their blending gives rather good results in practice compared with using, for instance, the ratio  $K/S$  calculated by the Kubelka-Munk theory. To me, Kubelka-Munk formulation is not the best way; one can find many other methods.

One point more about Dr Wahren's observation on the mean free path of the photon. When you attempt to study the transfer of radiations in diffusing media such as paper by corpuscular methods (as we did\*), it is useful to compare the thickness of the sheet of paper with the mean free path for scattering of the photon. This mean free path is a few microns—that is, on average, about one tenth of the thickness of a sheet of paper. If the sheet is thinner than the value of two or three mean free paths, it is easy to understand that the corpuscular theory is no more valuable for explaining the diffusing process of light in the paper than is the Kubelka-Munk theory. In

\* Silvy, J. *Rev. d'Optique Théorique et Instrumentale*, 1970, **40** (10), 495–517

fact, this morning, with the contribution on the printing properties of paper, we have seen results interpreted with Kubelka-Munk formulae and we could see from the graphs that the agreement between theory and practice is not good for thin papers, though better for thicker papers.

*Mr N. C. Underwood* Would Mr Hall tell us whether the instrument can be used with coloured papers; also, on higher grammages, whether the non-linearity of the absorption of the paper with respect to grammage is compensated for in the circuitry of the equipment.

*Mr Hall* We have not tried it on coloured paper at all. I guess the question is does the colour dictate formation? I cannot at the moment see that it will. So far as the mean opacity is concerned, the instrument in fact compensates for it by measuring mean opacity and correcting the gain, so that the point of operation is always normalised for opacities up to grammages of 60 or 80 g/m<sup>2</sup>. Of course, with higher weight materials, less light is transmitted, because the gain has increased and the accuracy is decreased owing to increasing noise in the system.

*Dr J. A. Van den Akker* My few comments are in favour of Kubelka and Munk. To begin with, if we got as good accuracy in our other fields of work on comparing theory with experiment as we do with Kubelka and Munk, we would all be delighted.

In 1967, I prepared an analysis that was presented at a symposium (conducted by the American Chemistry Society in Chicago) on reflectance spectroscopy.\* The purpose of that analysis was to discuss the discrepancies exhibited by the Kubelka-Munk theory, such as the interaction between scattering and absorption coefficients. I utilised a mathematical approach worked out 100 years ago by a famous English physicist, G. G. Stokes. Stokes analysed the problem of parallel plates very thoroughly and rigorously. This permitted me to set up a model of parallel layers to study the reflection of light from the model and to make variations in the disposition of the absorbing material and the scattering sites (in this case, interfaces). The results could be compared with the Kubelka-Munk equations to obtain equivalent values of the scattering coefficient.

It was shown that indeed the apparent discrepancies of the Kubelka-Munk theory depend on the exact model that one chooses. The model implied by the Kubelka-Munk theory is presented at the outset of the paper referred to. For that model, the Kubelka-Munk theory is *rigorously correct*—real systems like paper and paper coatings deviate in varying degrees from the idealised

\* Published as *Modern Aspects of Reflectance Spectroscopy*, edited W. W. Wendlandt (Plenum Press, New York, 1968), 27–46

## Discussion

model, resulting in various degrees of error. I disagree that the scattering coefficient is an artefact.

From a strictly operational point of view, one can take a small thickness of *any* medium and talk about the relative back scattering from the layers of radiation, light, cosmic rays, etc., using the same kind of double differential coefficients that were worked out years ago by Kubelka and Munk. One can express the *relative* back-scattered radiation as the scattering coefficient times the increment of thickness or grammage. To me, it is no matter that we have an exact fit of the model to the ideal, so long as on average we have a fairly good distribution of light-scattering sites throughout a reasonable area of the medium. The scattering coefficient then takes on a definable meaning.

*The Chairman* Most of us here are well aware of the caution to be exercised when using parameters extracted from mathematical models.

*Dr A. M. Scallan* In view of the statements concerning both the Kubelka-Munk theory and our theory, I would like to show a diagram in which the two theories are superimposed (Fig. U). It is seen that, apart from differences in units, the two theories agree over the most useful range of optical properties, in that the trends shown by  $k$  and  $s$  are duplicated by  $a$  and  $t$ , respectively. It would therefore appear that, despite the two very different approaches, the two theories are mutually supporting rather than opposing. Perhaps what our approach will prove useful for in the future is to give us a

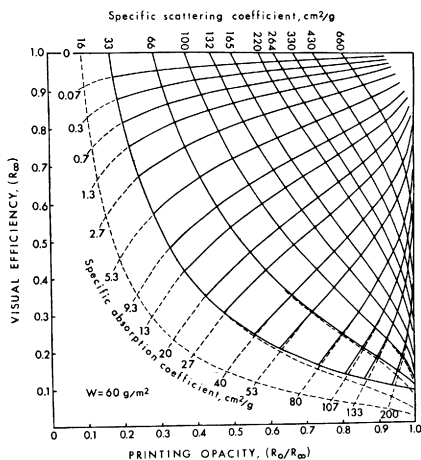


**Fig. U**—The superimposition of the Kubelka-Munk theory (broken lines) upon the theoretical lines of the layer theory presented by Scallan & Borch (see Fig. 1 of their paper, p. 156)



better knowledge of what  $s$  and  $k$  are in terms of tangible structural parameters, these being attainable from  $s$  and  $k$  through conversion factors.

*Prof. Wahren* Just a word of caution on the measurement of reflectance and transmission factors on non-uniform papers. This problem is treated by Norman and myself in our paper. It is stated by Dr Corte, also by Larsson & Trollsås that the Kubelka-Munk theory is strictly valid only if the measurement is performed on a sufficiently large area. This is not true for non-uniform papers. In fact, the theory, if valid at all, should be so only locally. The total reflectance or transmission should then be integrated over the area. This gives rise to rather non-linear relations for non-uniform papers.

*Dr H. Corte* Not only does the Kubelka-Munk formalism apply solely when conditions are satisfied that Kubelka and Munk stated very clearly: there is at least one more condition and that is the absence of optical anisotropy. This did not occur to Kubelka and Munk, because they were then (so far as I know) working at the Czechoslovakian Paint Research Institute, Aussig (1931, now Usti) and their coats of pigment paint did not show anisotropy. With highly oriented paper, however, you can observe some interesting effects such as elliptic scattering figures that can be changed with a polariser and that depend also on the wavelength. The scattering circle produced by a 1 mm  $\times$  1mm aperture indicates uniform radiation intensities over small distances inside the circle, but not that the paper is uniform. It is nothing but an edge effect. With a 100 micron or 1 micron aperture, the effect is even more drastic. I observed that, with a 100 micron aperture, the enlargement of the image through a 100 g/m<sup>2</sup> paper is not 2½ times as shown here, but 5 or 6 times.

*Mr J. R. Parker* It may be generally known that the translucency effect is of importance to the printing quality of paper. There is a reference <sup>(21)</sup> to this effect in Dr Karttunen's paper.

*Prof. H. W. Giertz* I wish to go back to this question of recalculating scattering in layers. I think this very dangerous to do with such a substance as paper. Scattering says nothing about the way in which light is scattered, but, to calculate the number of layers, I think papermakers will think actually in layers of the sheet. For instance, on newsprint, the scattering coefficient is 700, which is just due to a lot of fine materials; it has no meaning to speak about layers. Take an ordinary paper from beaten pulp: dried from water, it has a scattering of 200. Calculation indicates a few layers. The same paper, when dried from liquid nitrogen without any shrinkage, has a scattering coefficient of 1 000. You would expect such a paper to have a very large number

### *Discussion*

of layers, but it has the same number of fibres as the sheet dried from water and it cannot have many more layers. The high scattering coefficient is only because of the fibrils formed in beating. We should be very careful therefore when transferring scattering in layers.

*Mr C. M. W. Wilson* This may be a question for Mr Hall or just an observation. We seem to be going in two directions: on the one hand, we are designing formation meters that take more and more account of these various subjective factors discussed this afternoon; on the other hand, we were also discussing formation measurements earlier in the week that are specifically designed to correlate with hydrodynamic and other phenomena on the wet ends of papermachines. As with all paper properties, I suppose the most important thing to the customer is that it shall stay the same and not vary rather than that it shall correlate very closely with visual judgments. As someone whose main efforts in life are devoted to making papermachines do the right thing, I am fairly sure that I would prefer the formation meter whose output is directly relatable to such things as turbulence in the flow box.